Electronic Supplementary Material (ESI) for Journal of Materials Chemistry A.

Supporting Information

The construction of a photocatalytic fuel cell based on piezoelectric-enhanced dual heterojunctions of PVDF-HFP supported 2D/3D composites toward photocatalytic degradation of tetracycline

Tingting Yu[a,*], Bing Yang[a], Ran Deng[a], Tao Yang[a], Jizhou Jiang[b,*]

[a]School of Environmental and Chemical Engineering, Jiangsu Ocean University, Lianyungang 222005, PR China.

[b]School of Environmental Ecology and Biological Engineering, Key Laboratory of Green Chemical Engineering Process of Ministry of Education, Engineering Research Center of Phosphorus Resources Development and Utilization of Ministry of Education, Novel Catalytic Materials of Hubei Engineering Research Center, Wuhan Institute of Technology, Wuhan 430205, China.

*Corresponding author's email: ting@jou.edu.cn (T. Yu); 027wit@163.com (J. Jiang)

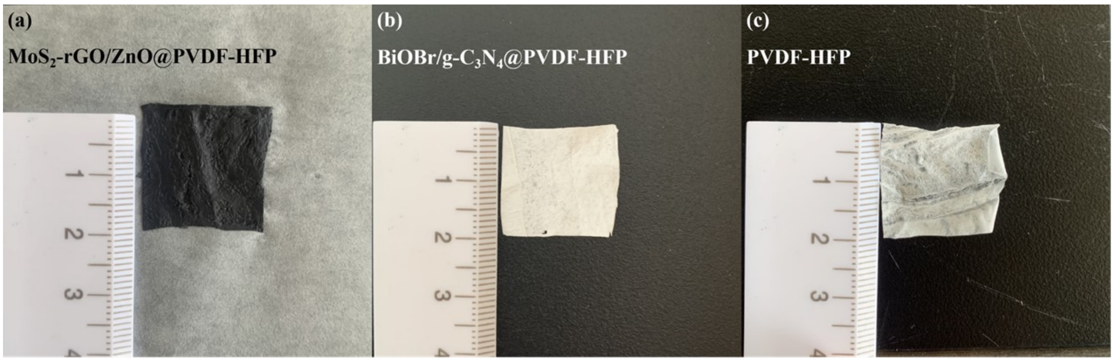

Fig. S1 Photos of (a) MoS$_2$-rGO/ZnO@PVDF-HFP, (b) BiOBr/g-C$_3$N$_4$@PVDF-HFP, and (c) PVDF-HFP.

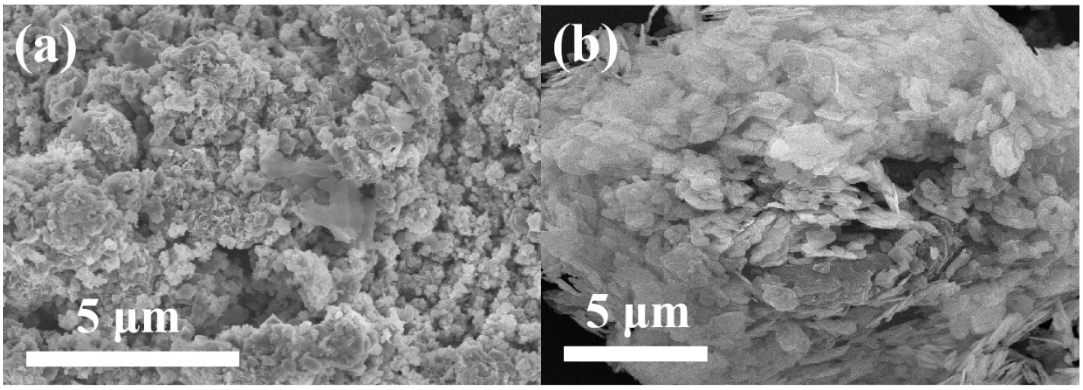

Fig. S2 SEM images of PFC after material cycling at two poles: (a) MoS_2-rGO/ZnO@PVDF-HFP, (b) BiOBr/g-C_3N_4@PVDF-HFP.

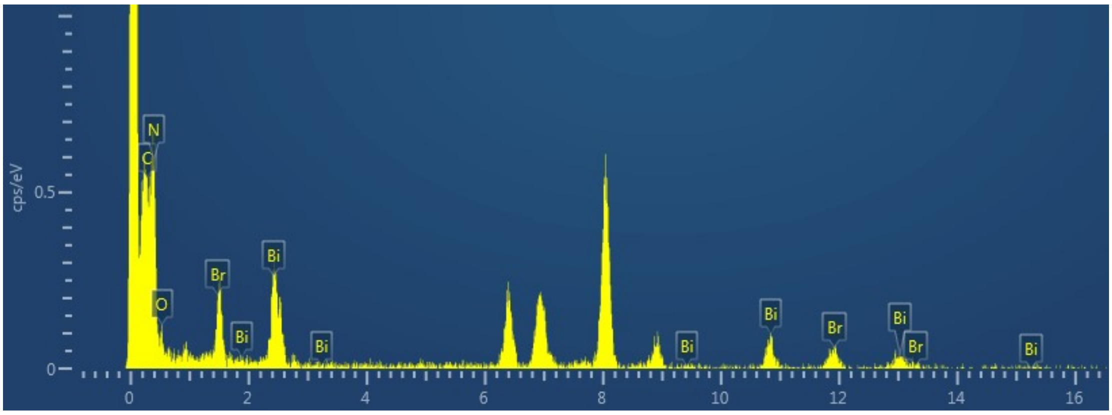

Fig. S3 EDS analysis of the BiOBr/g-C_3N_4 composite displays the intensity of elements such as C, N, Bi, Oand Br.

Table S1 Pore properties and BET surface area data. (Adsorbent: N_2, temperature: 150°C, instrument model: BSD-PM).

Catalysts	BET surface area (m^2 g^{-1})	Pore volume (cm^3 g^{-1})	Pore size (nm)
MoS_2	9.8248	0.0572	23.2880
MoS_2-rGO	20.3196	0.1264	24.8824
ZnO	10.2412	0.0818	31.9494
MoS_2-rGO/ZnO	28.219	0.1814	25.71
g-C_3N_4	25.1027	0.1796	28.6184
BiOBr	5.8179	0.0402	27.6388
BiOBr/g-C_3N_4	8.9615	0.0843	37.6276

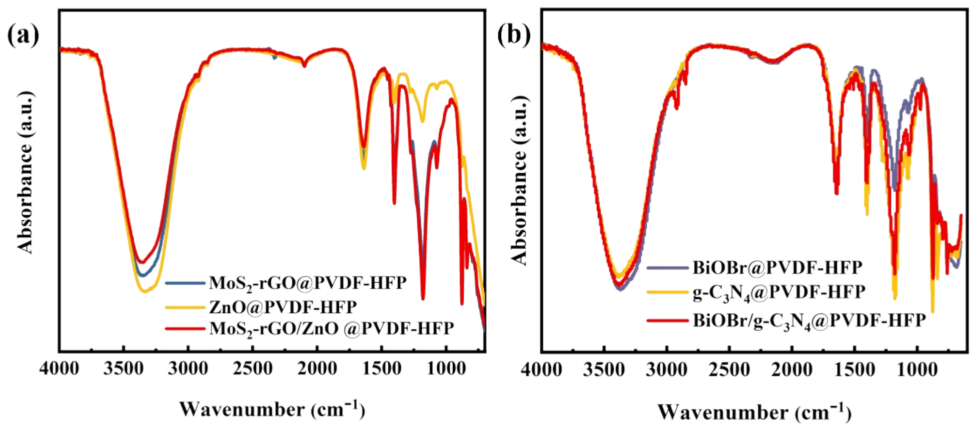

Fig. S4 FT-IR full spectra.

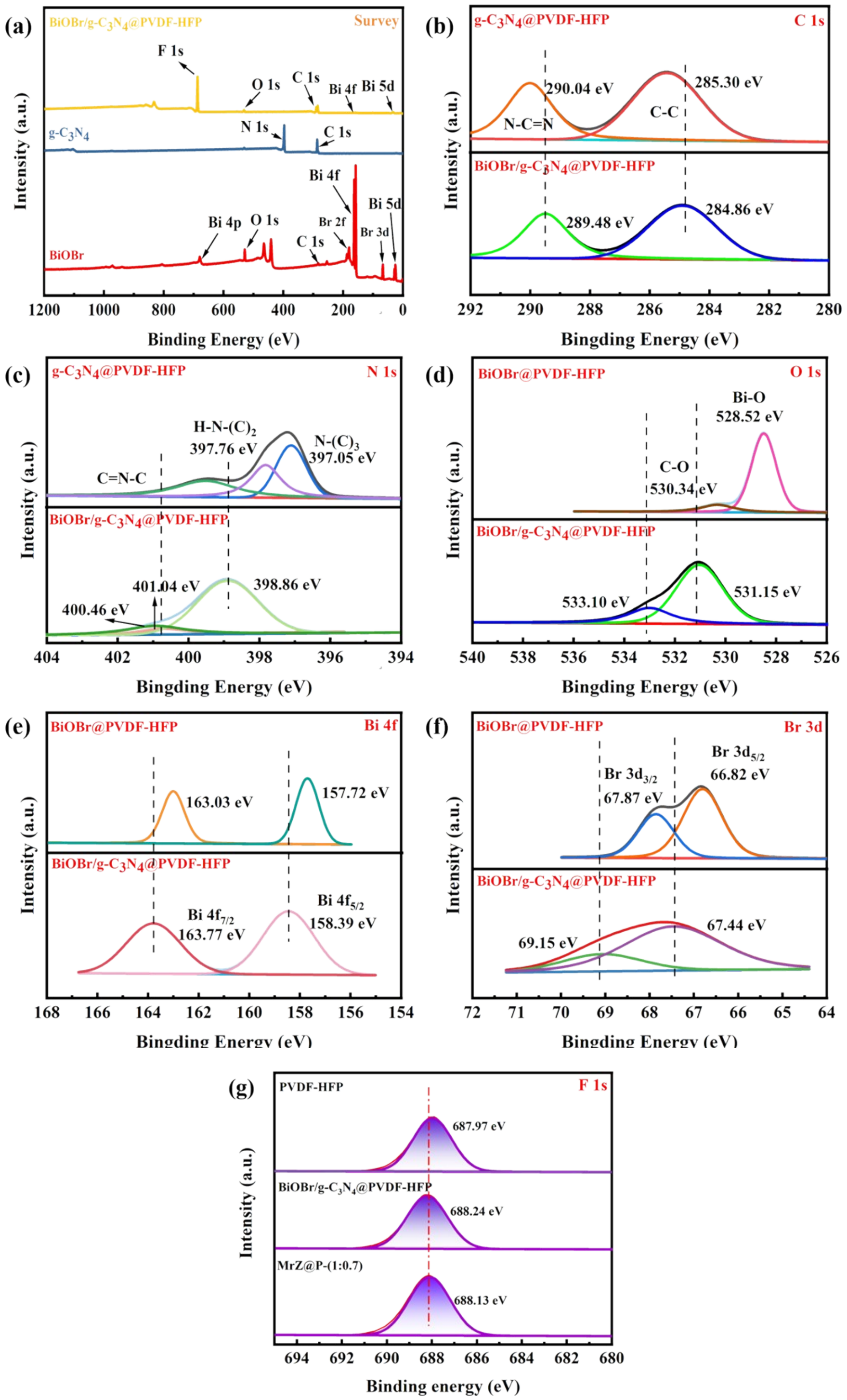

Fig. S5 (a) Full spectra of XPS: single material and composite material before and after degradation. (b) C1s, (c) N 1s, (d) O 1s, (e) Bi 4f, (f) Br 3d, (g) F 1s.

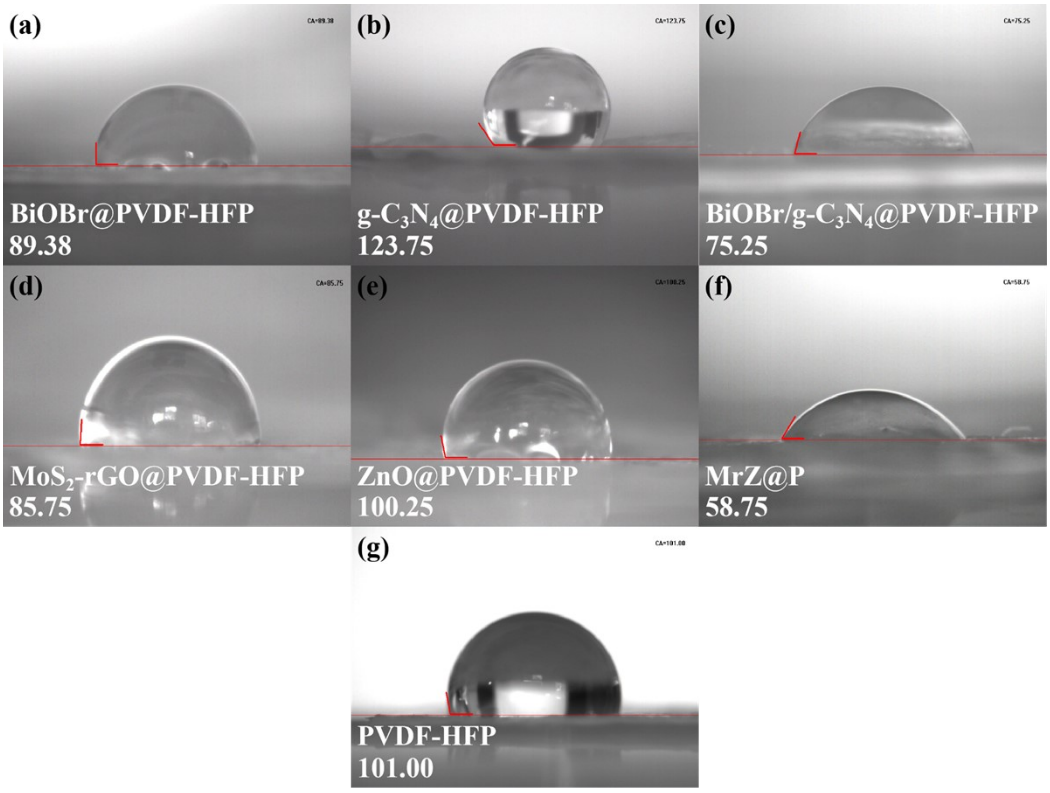

Fig. S6 Water contact angles.

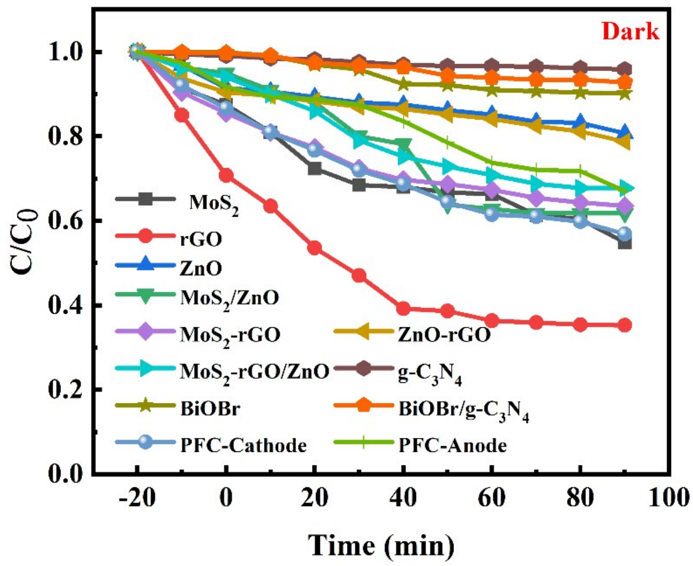

Fig. S7 Adsorption of TC by different materials during 110 minutes of dark standing.

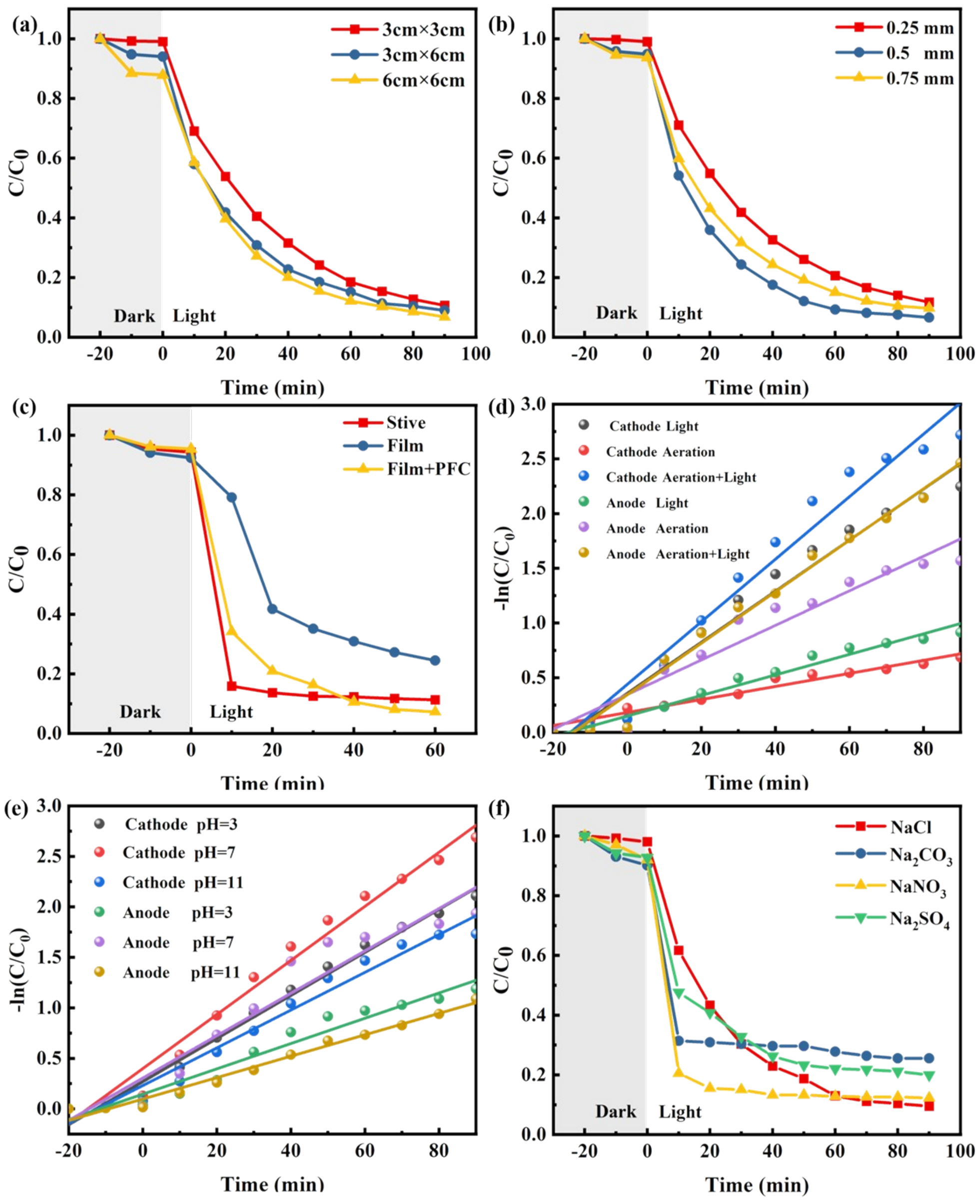

Fig. S8 Exploration conditions of photocatalytic properties: (a) influence of membrane area size on TC degradation rate, (b) film thickness, (c) system construction. Pseudo-first-order kinetic curve of degradation rate: (d) Piezoelectric illumination factor; (e) pH. (f) Effect of different anions on TC degradation rate in water.

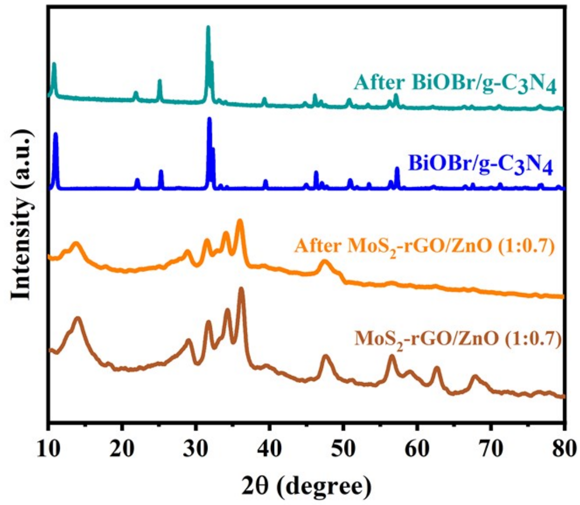

Fig. S9 XRD patterns of bipolar materials after 5 cycles of photocatalytic degradation of TC.

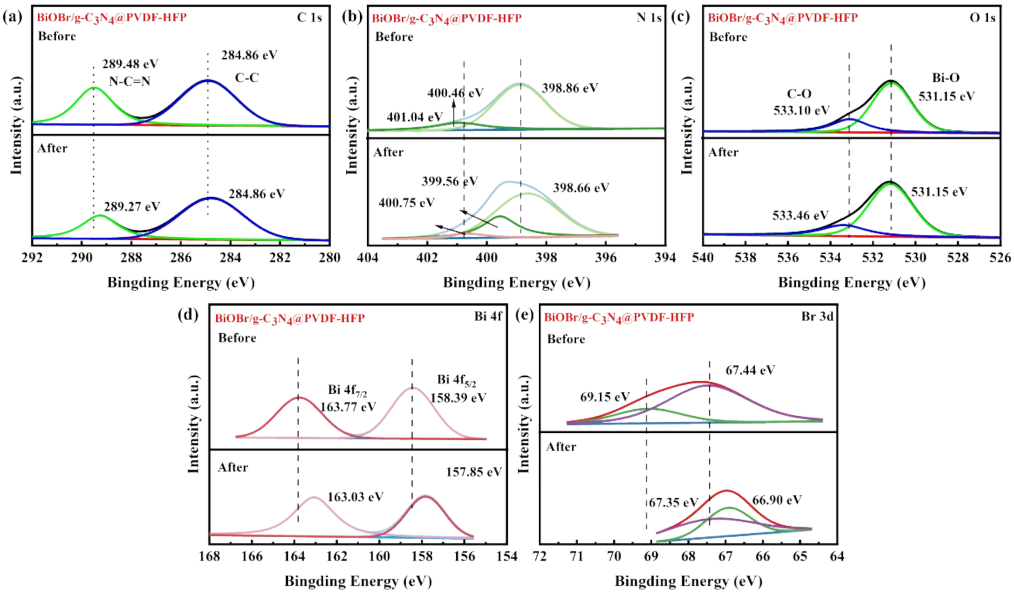

Fig. S10 XPS spectra of cathode material before and after cycle: (a) C1s, (b) N 1s, (c) O 1s, (d) Bi 4f, (e) Br 3d.

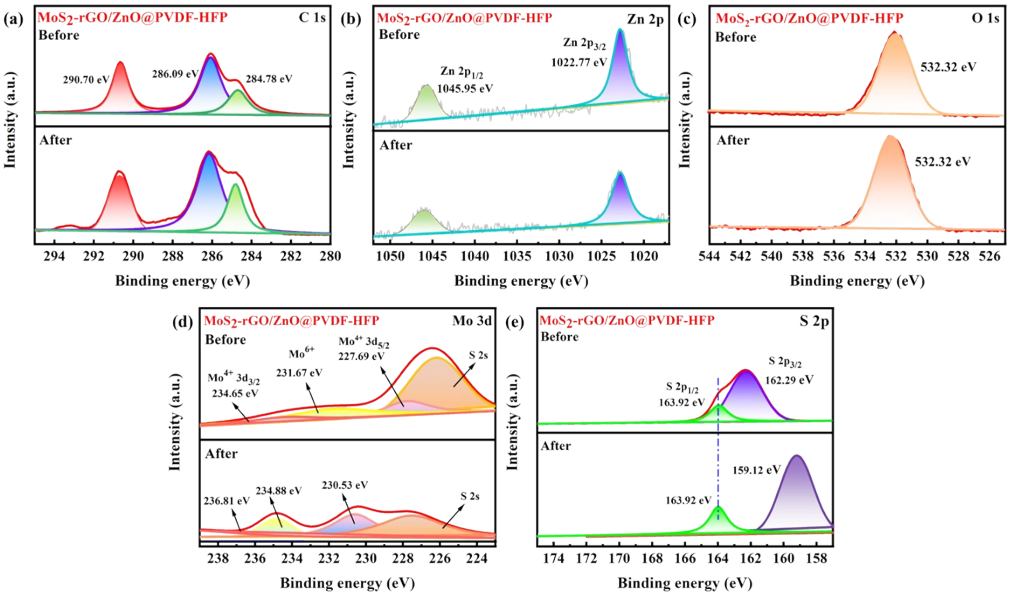

Fig. S11 XPS spectra of anode material before and after cycle: (a) C 1s, (b) Zn 2p, (c) O 1s, (d) Mo 3d, (e) S 2p.

Table S2 Statistics of TOC removal rate of pollutants by electrode materials in different PFC systems. (Pollutant: TC).

Cathode	Anode	Concentration ($mg\cdot L^{-1}$)	Time	TOC (%)	Ref.
Pt	TiO_2/Ti	20	60	34.87	[57]
TiO_2/BJS	Fe-$NiCo_2S_4$	45	90	74.12	[20]
Pt	Cr-BOC/Ag	20	120	54.37	[9]
CuCoCe	CQDs-TiO_2	45	60	75	[3]
WO_3	g-C_3N_4/FeO(1%)/TiO_2	10	90	65.4	[58]
Pt	Si PVC/ STNR	20	360	63.4	[59]
MoS_2-rGO/ZnO@PVDF-HFP	BiOBr/g-C_3N_4@PVDF-HFP	20	90	85.61	This work

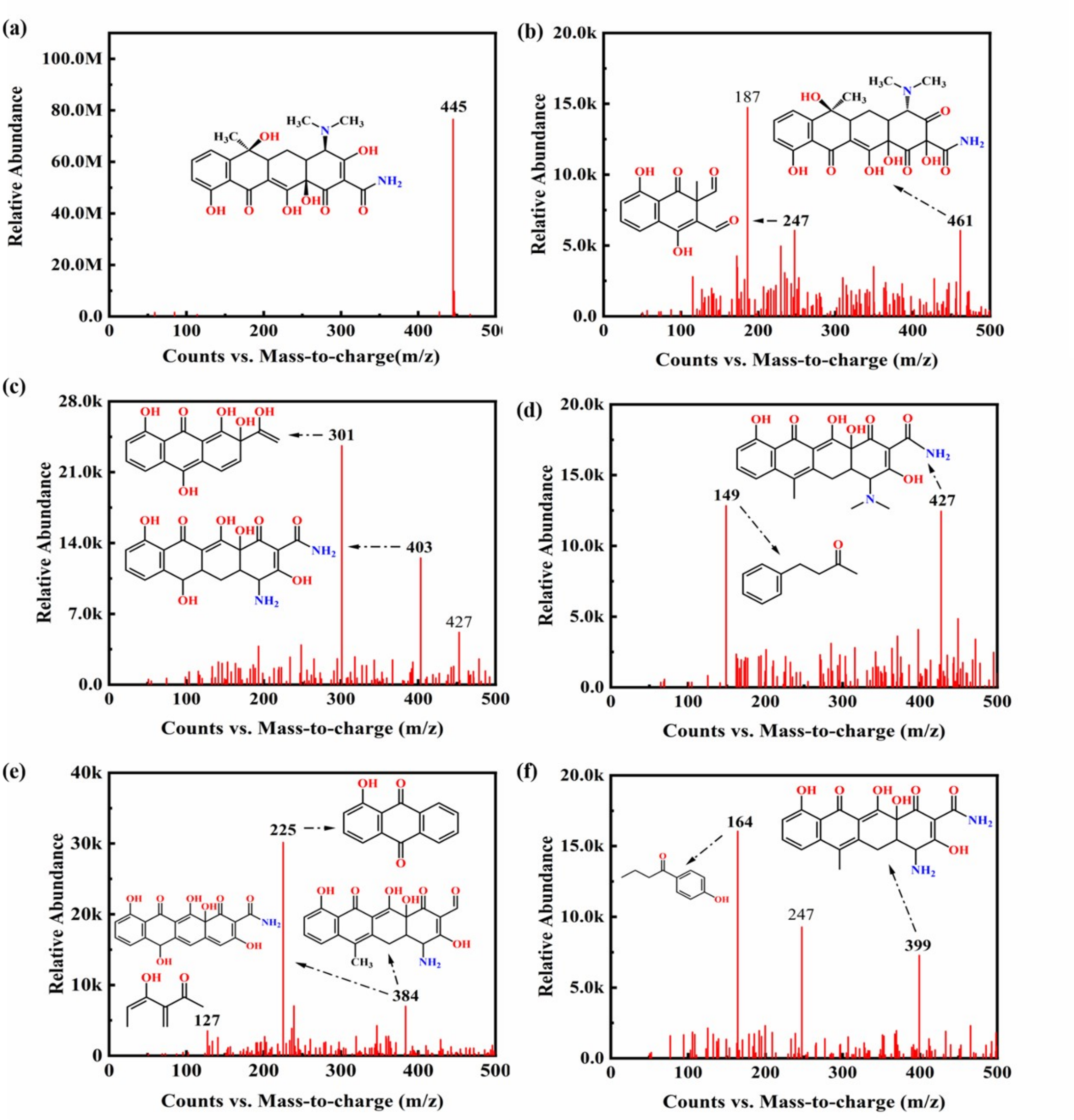

Fig. S12 MoS_2-rGO/ZnO@PVDF-HFP (1:0.7) m/z value of TC degradation. (TC solution before degradation (a) and at different times within 90 min (b-f)).